

AD-A047 923

AIR FORCE GEOPHYSICS LAB HANSCOM AFB MASS

F/6 4/1

SUNRISE E-REGION ENHANCEMENTS FROM AURORALLY INCREASED NO: THEO--ETC(U)

SEP 77 W SWIDER, T J KENESHEA, C I FOLEY

UNCLASSIFIED

AFGL-TR-77-0204

NL

| OF |

AD
A047923



END
DATE
FILMED
1 -78
DDC

AD A047923

14

AFGL-TR-77-0204, AFGL-ERP-648
ENVIRONMENTAL RESEARCH PAPERS, NO. 608

12

9

Final rept.,



6

Sunrise E-Region Enhancements From
Aurorally Increased NO: Theory.

10

WILLIAM / SWIDER,
THOMAS J. / KENESHEA
CAROL J. / FOLEY

11

15 Sept 1977

12

23 p.

DDC
RECEIVED
DEC 29 1977
B

16

6690

17

06

Approved for public release; distribution unlimited.

AERONOMY DIVISION PROJECT 6690

AIR FORCE GEOPHYSICS LABORATORY

HANSCOM AFB, MASSACHUSETTS 01731

AIR FORCE SYSTEMS COMMAND, USAF



AD No.

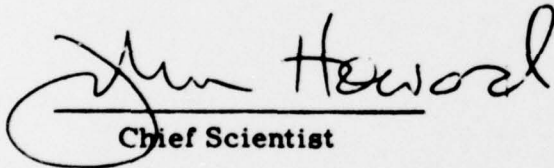
DDC FILE COPY

409 578

This report has been reviewed by the ESD Information Office (OI) and is releasable to the National Technical Information Service (NTIS).

This technical report has been reviewed and is approved for publication.

FOR THE COMMANDER


Chief Scientist

Qualified requestors may obtain additional copies from the Defense Documentation Center. All others should apply to the National Technical Information Service.

Unclassified

SECURITY CLASSIFICATION OF THIS PAGE (When Data Entered)

REPORT DOCUMENTATION PAGE		READ INSTRUCTIONS BEFORE COMPLETING FORM
1. REPORT NUMBER AFGL-TR-77-0204 ✓	2. GOVT ACCESSION NO.	3. RECIPIENT'S CATALOG NUMBER
4. TITLE (and Subtitle) SUNRISE E-REGION ENHANCEMENTS FROM AURORALLY INCREASED NO _x THEORY		5. TYPE OF REPORT & PERIOD COVERED Scientific Final
7. AUTHOR(s) William Swider Thomas J. Keneshea Carol I. Foley*		6. PERFORMING ORG. REPORT NUMBER ERP, No. 608 ✓
9. PERFORMING ORGANIZATION NAME AND ADDRESS Air Force Geophysics Laboratory (LKB) Hanscom AFB Massachusetts 01731 ✓		8. CONTRACT OR GRANT NUMBER(s)
11. CONTROLLING OFFICE NAME AND ADDRESS Air Force Geophysics Laboratory (LKB) Hanscom AFB Massachusetts 01731		10. PROGRAM ELEMENT, PROJECT, TASK AREA & WORK UNIT NUMBERS 62101F 66900601
14. MONITORING AGENCY NAME & ADDRESS (if different from Controlling Office)		12. REPORT DATE 15 September 1977
		13. NUMBER OF PAGES 23
		15. SECURITY CLASS. (of this report) Unclassified
		15a. DECLASSIFICATION/DOWNGRADING SCHEDULE
16. DISTRIBUTION STATEMENT (of this Report) Approved for public release; distribution unlimited.		
17. DISTRIBUTION STATEMENT (of the abstract entered in Block 20, if different from Report)		
18. SUPPLEMENTARY NOTES * Boston College		
19. KEY WORDS (Continue on reverse side if necessary and identify by block number) E-region ionization Aurora Nitric oxide in aurora Sunrise E-region Disturbed E-region		
20. ABSTRACT (Continue on reverse side if necessary and identify by block number) E-region nitric oxide concentrations are known to be greater at high altitudes as compared to low- and midlatitudes. It is suggested that studies of electron concentration data from ionosondes and/or the Chatanika backscatter radar at night, and especially at sunrise, may be able to provide peak nitric oxide concentrations when aurora are determined to be absent.		

DD FORM 1 JAN 73 1473 EDITION OF 1 NOV 65 IS OBSOLETE

Unclassified

SECURITY CLASSIFICATION OF THIS PAGE (When Data Entered)

Preface

The work contained in this report was originally presented, in less detail, at the December 1977 American Geophysical Union meeting in San Francisco, California.

ACCESSION for		
NTIS	White Section	<input checked="" type="checkbox"/>
DDC	Buff Section	<input type="checkbox"/>
UNANNOUNCED		<input type="checkbox"/>
JUSTIFICATION		
BY		
DISTRIBUTION/AVAILABILITY CODES		
Dist.	AVAIL	and/or SPECIAL
A		

Contents

1. INTRODUCTION	7
2. CALCULATIONS	8
3. DISCUSSION	10
REFERENCES	23

Illustrations

1a. Ionization Production Rates for NO^+ From $\text{H}\gamma\alpha$ at Sunrise (Sunset) vs Altitude for Selected Solar Zenith Angles	12
1b. Ionization Production Rates for NO^+ From $\text{H}\gamma\alpha$ at Sunrise (Sunset) vs Solar Zenith Angle for Selected Altitudes	12
2a. Sunrise Electron Concentration Profiles vs Altitude for Selected Solar Zenith Angles From 98° to 86°	13
2b. Sunrise Electron Concentration Profiles vs Solar Zenith Angles for Selected Altitudes From 85 to 140 km	13
3a. Same as for Figure 2a, Except NO Increased by a Factor of 10	14
3b. Same as for Figure 2b, Except NO Increased by a Factor of 10	14
4a. Same as for Figure 2a, Except NO Increased by a Factor of 10^2	15
4b. Same as for Figure 2b, Except NO Increased by a Factor of 10^2	15
5a. Same as for Figure 2a, Except NO Increased by a Factor of 10^3	16

Illustrations

5b. Same as for Figure 2b, Except NO Increased by a Factor of 10^3	16
6. Presunrise Electron Concentration Profiles for the Four Different NO Profiles Used	17
7. Electron Concentration Profiles at Ground Sunrise for the Four Cases	17
8. Same as Figure 6, Except Absorption of HLy α by NO Included	18
9. Same as Figure 7, Except Absorption of HLy α by NO Included	18
10a. Same as Figure 1a, Except NO Increased by a Factor of 10^2 and Absorption of HLy α by NO Included	19
10b. Same as Figure 1b, Except NO Increased by a Factor of 10^2 and Absorption of HLy α by NO Included	19
10c. Same as Figure 2a, Except NO Increased by a Factor of 10^2 and Absorption of HLy α by NO Included	20
10d. Same as Figure 2b, Except NO Increased by a Factor of 10^2 and Absorption of HLy α by NO Included	20
11a. Same as Figure 1a, Except NO Increased by a Factor of 10^3 and Absorption of HLy α by NO Included	21
11b. Same as Figure 1b, Except NO Increased by a Factor of 10^3 and Absorption of HLy α by NO Included	21
11c. Same as Figure 2a, Except NO Increased by a Factor of 10^3 and Absorption of HLy α by NO Included	22
11d. Same as Figure 2b, Except NO Increased by a Factor of 10^3 and Absorption of HLy α by NO Included	22

Table

1. Ionic E-region Processes	8
-----------------------------	---

Sunrise E-Region Enhancements From Aurorally Increased NO: Theory

1. INTRODUCTION

Nitric oxide is a minor, but important, constituent of the atmosphere up to approximately 150 km. This ubiquitous gas can contribute to ozone destruction in the stratosphere. In the E-region, the present subject, NO functions in several ways. In the normal daytime E-region, the role of nitric oxide is confined mainly to converting O_2^+ ions into NO^+ ions. These two ions are the major ionic species except in cases of sporadic-E layers which may consist primarily of metallic ions. The O_2^+ to NO^+ conversion process impacts upon the mean recombination coefficients in the E-region, but not in an overwhelming way, since the dissociative recombination rates of these species only differ by a factor of two. Nitric oxide has a more significant role at night¹ and twilight,² however, since this gas is ionized by solar hydrogen Lyman alpha radiation, $H\gamma\alpha$, which is present at night due to scattering effects, and because at twilight the direct solar $H\gamma\alpha$ photons easily penetrate into the lower E-region in contrast to radiation which ionizes O, O_2 , and N_2 .

(Received for publication 15 September 1977)

1. Nicolet, M. (1965) Ionospheric processes and nitric oxide, J. Geophys. Res. 70:691-701.
2. Swider, W. (1965) A study of the nighttime ionosphere and its reaction rates, J. Geophys. Res. 70:4859-4873.

2. CALCULATIONS

The nitric oxide profile adopted in the computations is that reported by Meira³ for 85-105 km, diffusive equilibrium being assumed for the higher altitudes. The specific values, in units of 10^7 cm^{-3} , were 1.5, 3.0, 6.0, 9.0, 10.0, 9.0, 5.12, 3.44, 2.64, 2.16, 1.79, 1.53, 1.3 and 1.13 for altitudes 85-150 km in 5 km intervals. The scattered radiation intensities for HLy α and HLy β at night are those chosen by Keneshea et al,⁴ namely 1 percent and 0.4 percent of the noon ($\chi = 45^\circ$) values for HLy α and HLy β , respectively. All other radiation intensities are as before⁴ except that X-rays are reduced 1/4. Neutral concentrations and temperatures were taken from the 1966 U. S. Standard Atmosphere Supplements for Fall-Spring at 45°N with a 1000°K exospheric temperature. Calculations were performed for 0° declination. Ionic reaction rates are listed in Table 1.

Table 1. Ionic E-region Processes

Reaction No.	Reaction	Rate Coefficient (cm^3/sec)
1.	$\text{O}_2^+ + e \rightarrow \text{O} + \text{O}$	$2.0 \times 10^{-7} (300/\text{T})$
2.	$\text{NO}^+ + e \rightarrow \text{N} + \text{O}$	$4.0 \times 10^{-7} (300/\text{T})$
3.	$\text{O}^+ + \text{O}_2 \rightarrow \text{O}_2^+ + \text{O}$	$1.5 \times 10^{-11} (300/\text{T})$
4.	$+ \text{N}_2 \rightarrow \text{NO}^+ + \text{N}$	$1.2 \times 10^{-12} (300/\text{T})$
6.	$\text{N}_2^+ + \text{O} \rightarrow \text{NO}^+ + \text{N}$	$1.5 \times 10^{-10} (300/\text{T})$
7.	$+ \text{O}_2 \rightarrow \text{O}_2^+ + \text{N}_2$	$5.0 \times 10^{-11} (300/\text{T})$
8.	$\text{N}^+ + \text{O}_2 \rightarrow \text{NO}^+ + \text{O}$	2.0×10^{-10}
9.	$+ \text{O}_2 \rightarrow \text{O}_2^+ + \text{N}$	4.0×10^{-10}
10.	$\text{O}_2^+ + \text{NO} \rightarrow \text{NO}^+ + \text{O}_2$	4.6×10^{-10}

3. Meira, L.G., Jr. (1971) Rocket measurements of upper atmospheric nitric oxide and their consequence to the lower ionosphere, *J. Geophys. Res.* 76:202-212.

4. Keneshea, T.J., Swider, W., and Narcisi, R.S. (1970) E-region model, *J. Geophys. Res.* 75:845-854.

Sunrise ionization production rates for NO^+ ions resulting from the ionization of NO by the direct $\text{HLY}\alpha$ line are shown in Figure 1a and, by a different format, in Figure 1b. Nighttime conditions are found to persist up to about $\chi = 98^\circ$ at sunrise, but by $\chi = 96^\circ$, the ionization of NO at 150 km has almost reached its maximum value. The resultant electron concentration, $[e]$, profiles are illustrated in Figures 2a and 2b. Note that equilibrium at 110 km is reached by $\chi = 90^\circ$. Figures 3a through 5b portray the same information for NO concentrations increased by $10\times$, $10^2\times$, and $10^3\times$. Respective ionization production rates are not shown since they are only like multiples of those rates in Figures 1a or 1b.

The main point we wish to stress is that since NO is known to be greater in the auroral zone⁵ as compared to low- and midlatitudes, the night and sunrise E-region at auroral latitudes may be more prominent than normal even in the absence of auroras. (The sunset E-region is also augmented over normal conditions, but will not be discussed here.) Figure 6 portrays the nighttime E-region in the case of "normal" NO and with NO increased by factors of 10, 10^2 , and 10^3 , an extreme limit. An ionosonde with a MHz threshold should observe the 10^2 case, especially since the scattered flux may be as much as a factor of two to three times greater⁶ than we assumed. Figure 7 depicts the situation for $\chi = 90^\circ$. All four situations now should be observable to an ionosonde with a 1 MHz threshold. Note, incidentally, that $[e] \approx [\text{NO}]^{1/2}$ near 110 km. Absorption of $\text{HLY}\alpha$ by NO has been neglected. Inclusion of this absorption has little impact upon the nighttime situation except for case 4, where a reduction of up to a factor of 2 in $[e]$ at the lowest altitude is attained (Figure 8). At $\chi = 90^\circ$, the change is much greater (Figure 9). For case 3, $[e]$ is reduced up to a factor of two near 100-110 km and the profile of $[e]$ for case 4 decreases from a factor of two near 150 km to almost a factor of 5 near 100-110 km. However, it is by no means certain that the inclusion of this absorption is more appropriate since higher concentration NO layers undoubtedly have a limited, if not extremely limited spatial extent, in comparison to the spherical symmetry assumed in the computations. Nevertheless, we present the effect of this absorption in Figures 10a-10d for case 3, and in Figures 11a-11d for case 4.

-
5. Rusch, D.W., and Barth, C.A. (1975) Satellite measurements of nitric oxide in the polar region, *J. Geophys. Res.* 80:3719-3721.
 6. Strobel, D.F., Young, T.R., Meier, R.R., Coffey, T.P., and Ali, A.W. (1974) The nighttime ionosphere: E-region and lower F-region, *J. Geophys. Res.* 79:3171-3178.

3. DISCUSSION

In any case, we propose that investigations of nonauroral high latitude ionosonde and/or Chatanika backscatter data at night, and especially at sunrise, may yield useful information in regards to NO enhancements. At night, it may be difficult to discriminate between a steady nighttime E-region due to ionization of enhanced [NO] in comparison to an E-layer produced by a weak but steady "drizzle" of precipitating electrons. Sporadic-E also may complicate the picture. Furthermore, a good knowledge of the actual scattered HLy α intensity at low altitudes is needed if [NO] is to be derived from ionosonde data for [e]. On the other hand, the unique signature of solar radiation at sunrise (Figure 1a, for example) produces a pattern (Figure 2a) that would be difficult for an electron precipitation event to reproduce. It is important to realize that although an ambient enhanced NO profile is likely different in shape from those adopted here, the peak value, which is of most interest, is the parameter which is to be correlated with ionosonde observations.

Wakai's⁷ survey of the nighttime E-region indicated enhanced E-layers in the auroral zone and polar cap even for quiet conditions. King,⁸ in a study of 197 auroras at night, reported three cases where $f_oE > 1.7$ MHz when overhead aurora appeared to be absent. The cases could be interpreted as indicating an NO layer peak of $\sim 3 \times 10^{10} \text{ cm}^{-3}$. Such high values have been reported by one rocket group.⁹ However, in a recent survey of all the other available (8) E-region auroral flights, Swider and Narcisi¹⁰ inferred NO layer peaks from 10^8 cm^{-3} to only 10^9 cm^{-3} . The difficulties in generating sufficient NO so as to equal the O₂ concentrations are well known and have recently been enumerated by Hyman et al.¹¹ Hopefully the more modest increases in nitric oxide, such as a peak concentration of 10^9 cm^{-3} , may be detectable at twilight from Chatanika backscatter and/or ionosonde data studies. Figure 3a illustrates this situation at sunrise. The [e] profiles are about a factor of 3 larger than that for "normal" conditions.

7. Wakai, N. (1967) Quiet and disturbed structure and variations of the nighttime E-region, *J. Geophys. Res.* 72:4507-4517.
8. King, G.A.M. (1965) The aurora and night E-layer, *J. Atmos. Terr. Phys.* 27:426-428.
9. Zipf, E.C., Borst, W.L., and Donahue, T.M. (1970) A mass spectrometer observation of NO in an auroral arc, *J. Geophys. Res.* 75:6371-6376.
10. Swider, W., and Narcisi, R.S. (1977) Auroral E-region: Ion composition and nitric oxide, *Planet. Space Sci.* 25:103-116.
11. Hyman, E., Strickland, D.J., Julienne, P.S., and Stroble, D.F. (1976) Auroral NO ?, *J. Geophys. Res.* 81:4765-4769.

We have not presented any sunset profiles because we believe a sunrise analysis would be preferable. For example, sunset decay of the E-region is likely to be perturbed more by sporadic-E. Furthermore, presunset auroral influences presumably are more difficult to discriminate from normal daytime E-region behavior in contrast to sunrise/nighttime circumstances.

Same IR effects may be of interest. The nitric oxide $\Delta\nu = 1$ system, radiates at $6.3 \mu\text{m}$. Its ion radiates at $4.3 \mu\text{m}$ ($\Delta\nu = 1$), which corresponds also to the 001-000 band wavelength of CO_2 . The possible sudden prominence of the NO^+ $4.3 \mu\text{m}$ band at sunrise due to the ionization of auroral/nuclear NO enhancements by the direct solar $\text{H}\gamma\alpha$ line, must not be confused with CO_2 emissions at the same IR wavelength. The natural (aurorally-caused) variations of NO and NO^+ at sunrise at high altitudes could be determined, as suggested by this paper, from appropriate ionosonde or Chatanika backscatter data. There may be enough sunrise ionosonde or Chatanika data (the latter stored at Stanford Research Institute) presently available, which could yield considerable information on the variation of NO^+ and NO at that particular auroral data site. We plan to investigate this possibility.

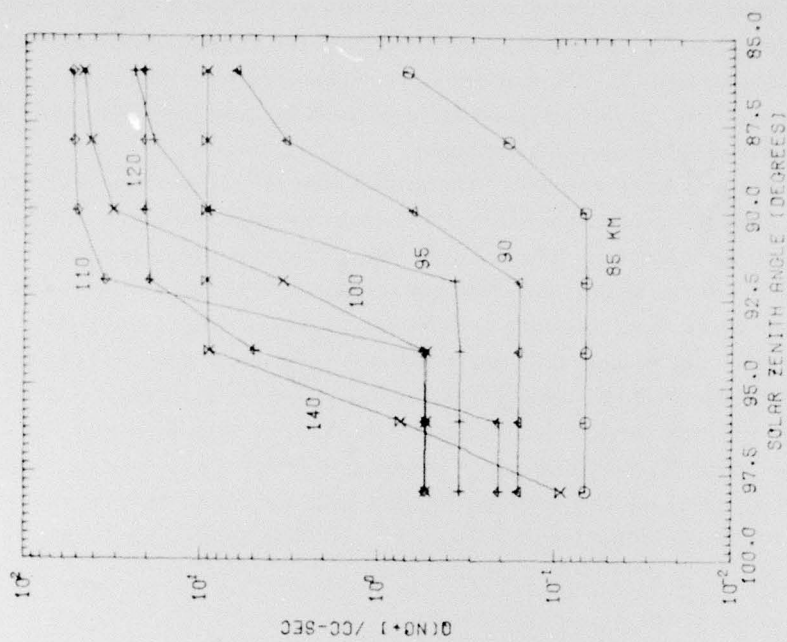


Figure 1a. Ionization Production Rates for NO^+ From $\text{HLY}\alpha$ at Sunrise (Sunset) vs Altitude for Selected Zenith Angles

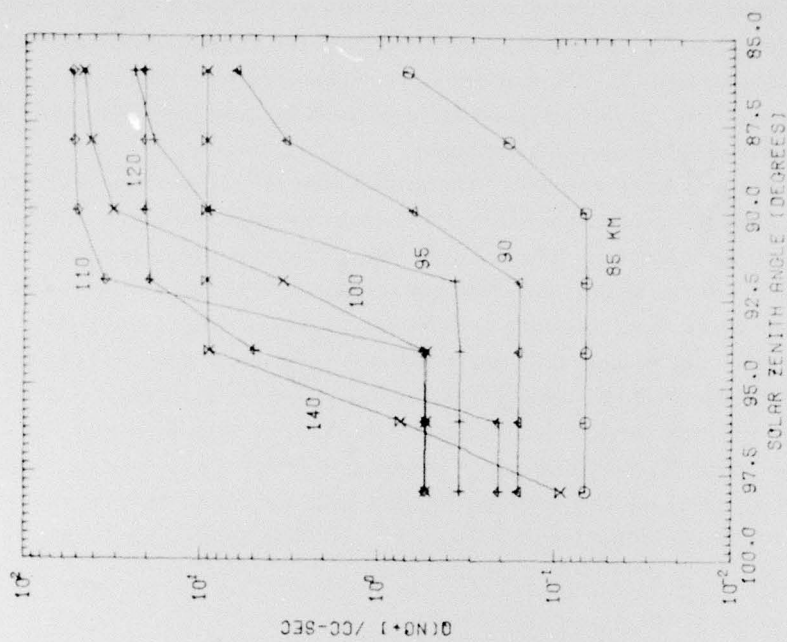


Figure 1b. Ionization Production Rates for NO^+ From $\text{HLY}\alpha$ at Sunrise (Sunset) vs Solar Zenith Angle for Selected Altitudes

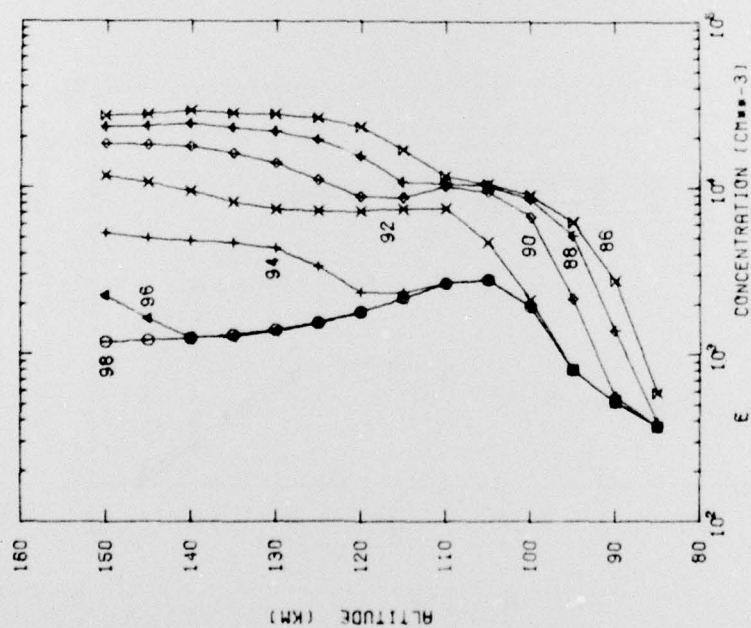


Figure 2a. Sunrise Electron Concentration Profiles vs Altitude for Selected Solar Zenith Angles From 98° to 86°

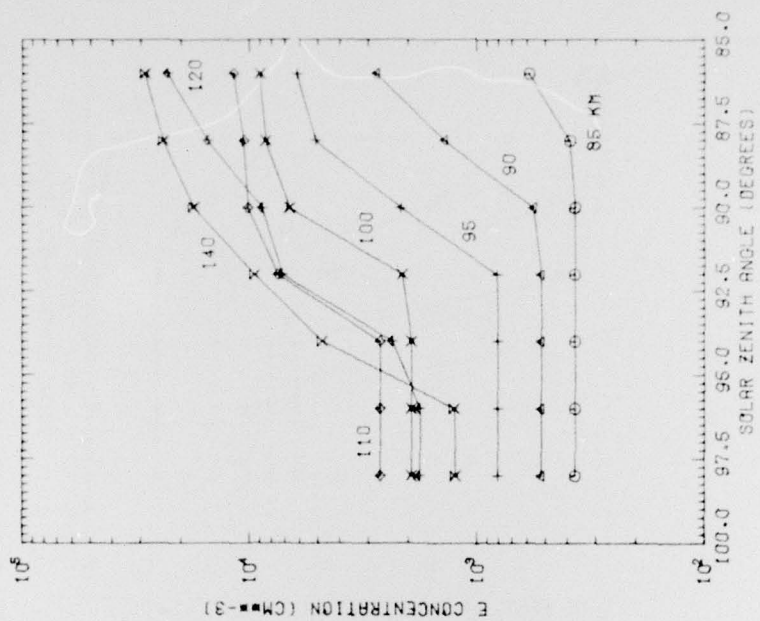


Figure 2b. Sunrise Electron Concentration Profiles vs Solar Zenith Angles for Selected Altitudes From 85 to 140 km

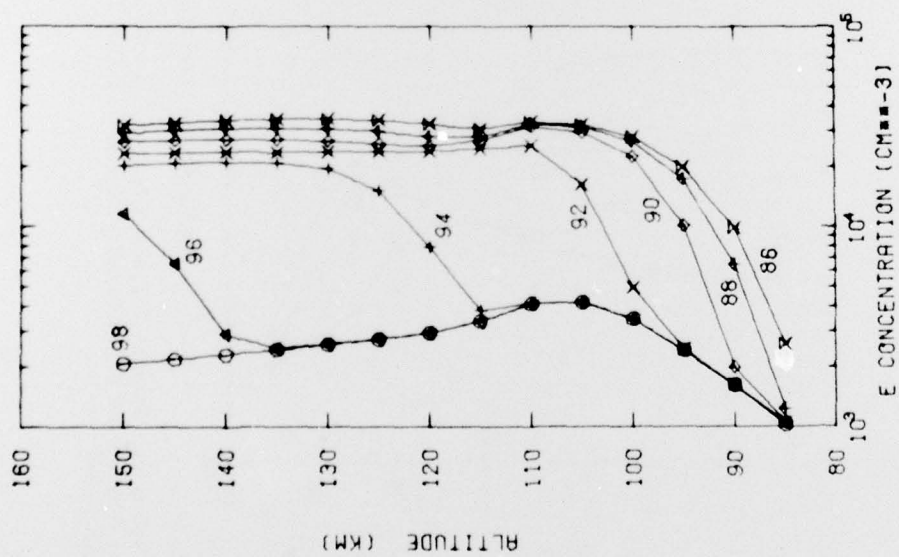


Figure 3a. Same as for Figure 2a, Except NO Increased by a Factor of 10

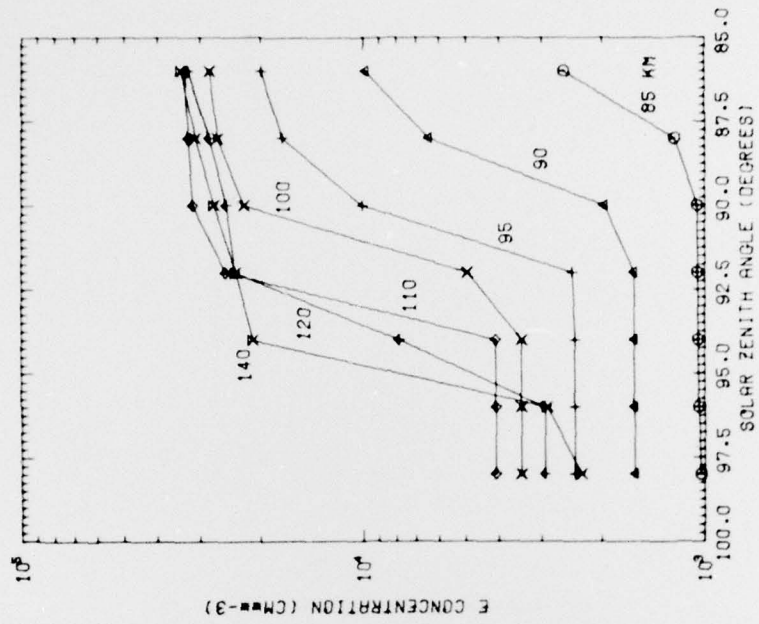


Figure 3b. Same as for Figure 2b, Except NO Increased by a Factor of 10

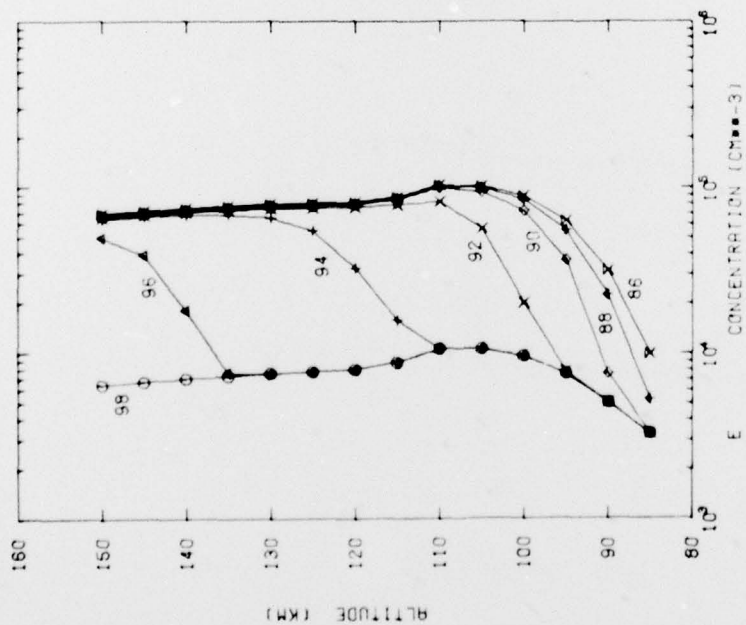


Figure 4a. Same as for Figure 2a, Except NO Increased by a Factor of 10^2

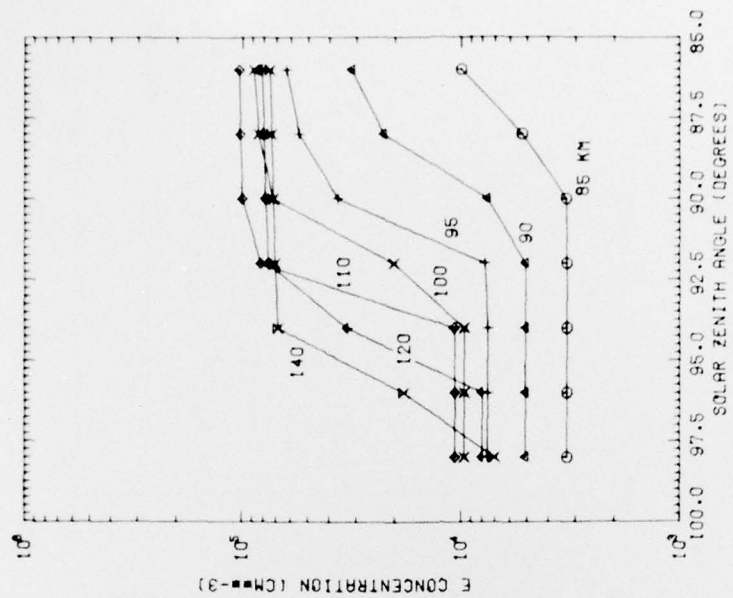


Figure 4b. Same as for Figure 2b, Except NO Increased by a Factor of 10^2

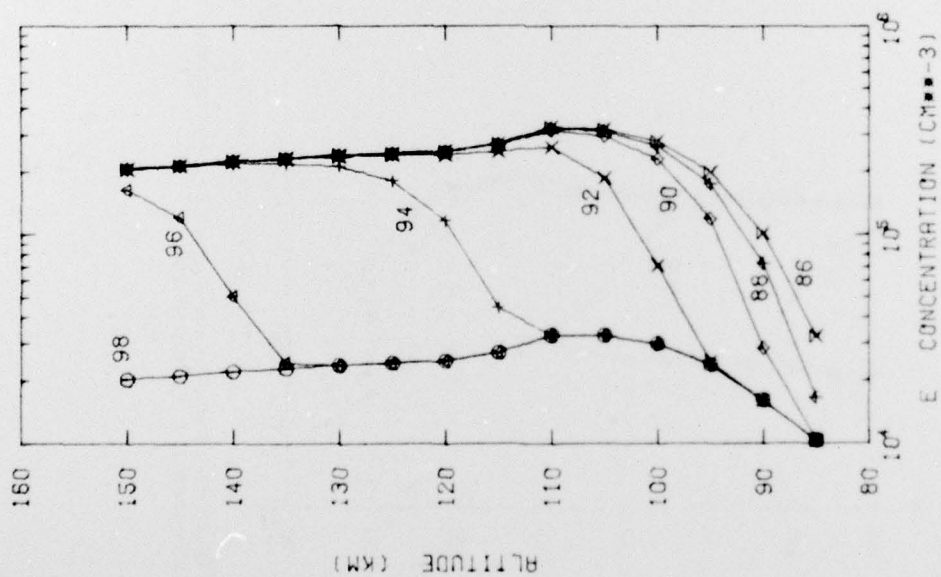


Figure 5a. Same as for Figure 2a, Except NO Increased by a Factor of 10^3

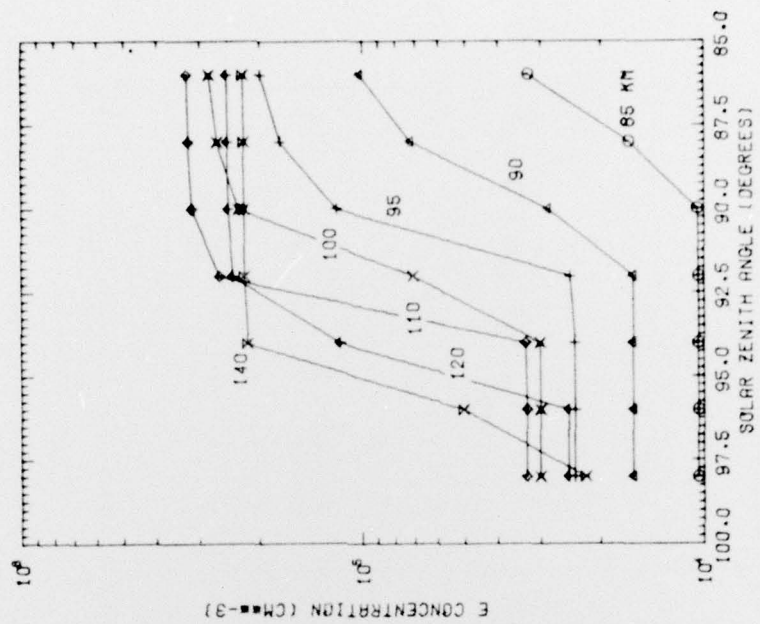


Figure 5b. Same as for Figure 2b, Except NO Increased by a Factor of 10^3

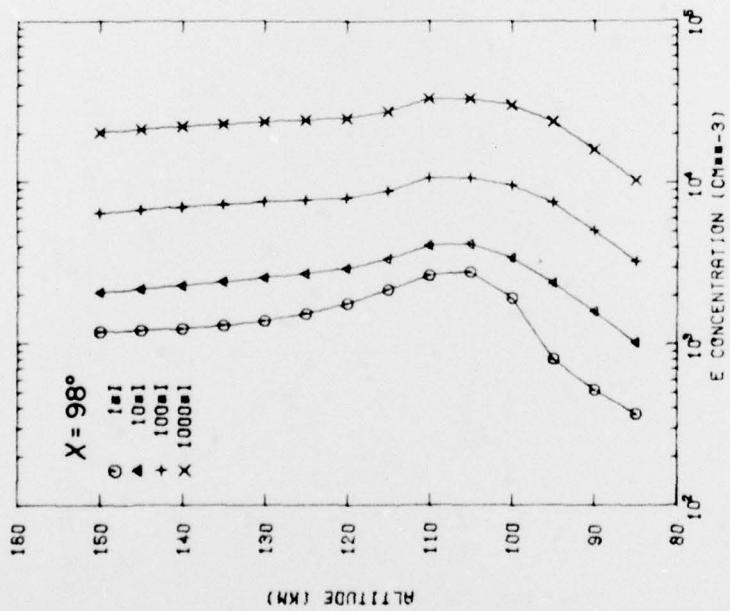


Figure 6. Presunrise Electron Concentration Profiles for the Four Different NO Profiles Used

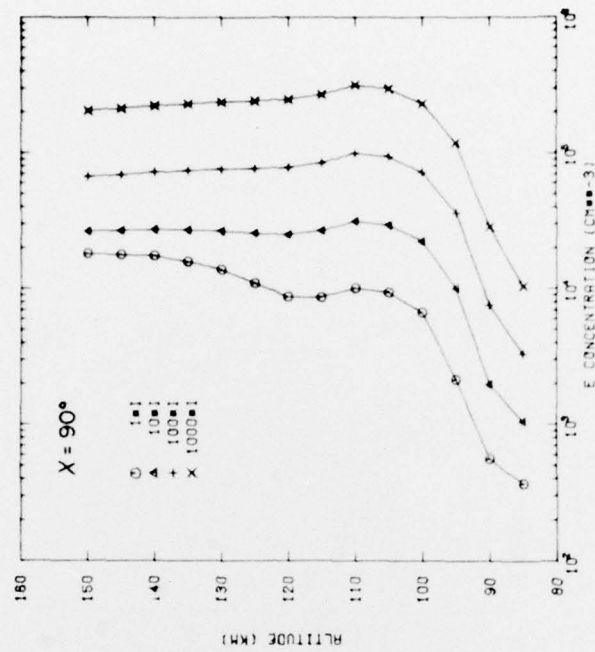


Figure 7. Electron Concentration Profiles at Ground Sunrise for the Four Cases

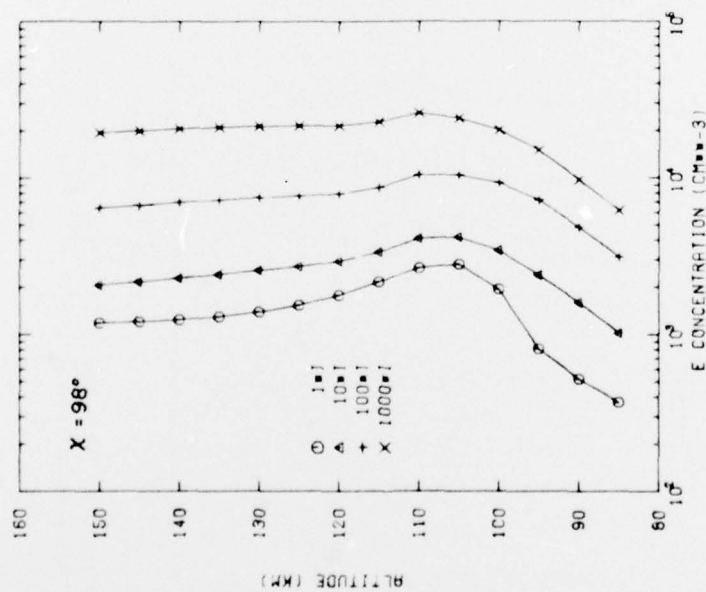


Figure 8. Same as Figure 6, Except Absorption of H_Lγ by NO Included

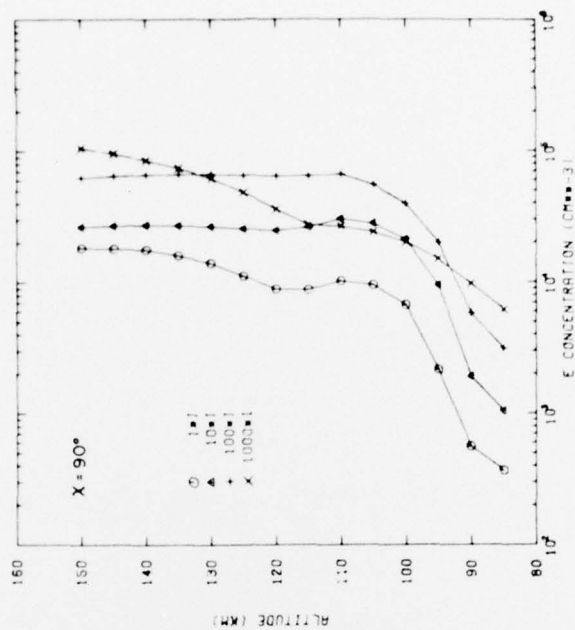


Figure 9. Same as Figure 7, Except Absorption of H_Lγ by NO Included

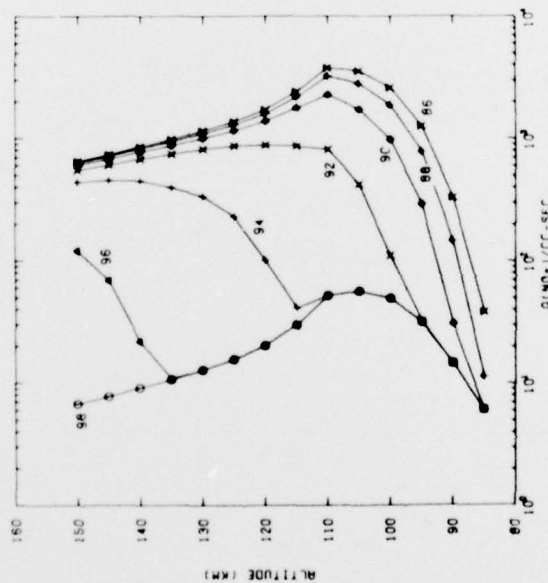


Figure 10a. Same as Figure 1a, Except NO Increased by a Factor of 10^2 and Absorption of $HL_{\gamma\alpha}$ by NO Included

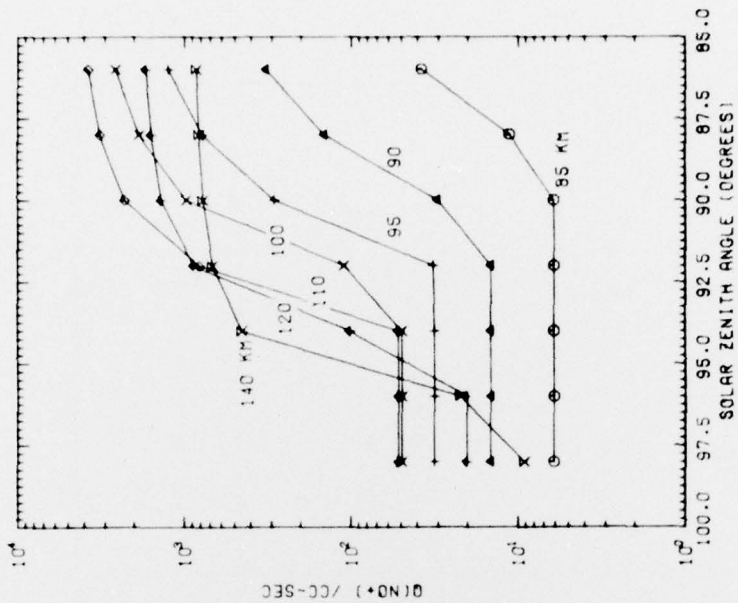


Figure 10b. Same as Figure 1b, Except NO Increased by a Factor of 10^2 and Absorption of $HL_{\gamma\alpha}$ by NO Included

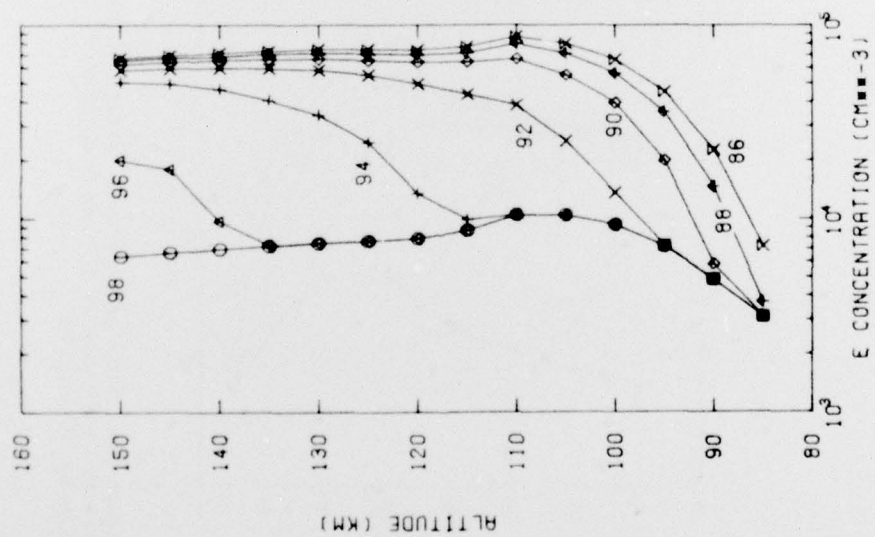


Figure 10c. Same as Figure 2a, Except NO Increased by a Factor of 10² and Absorption of HfLy α by NO Included

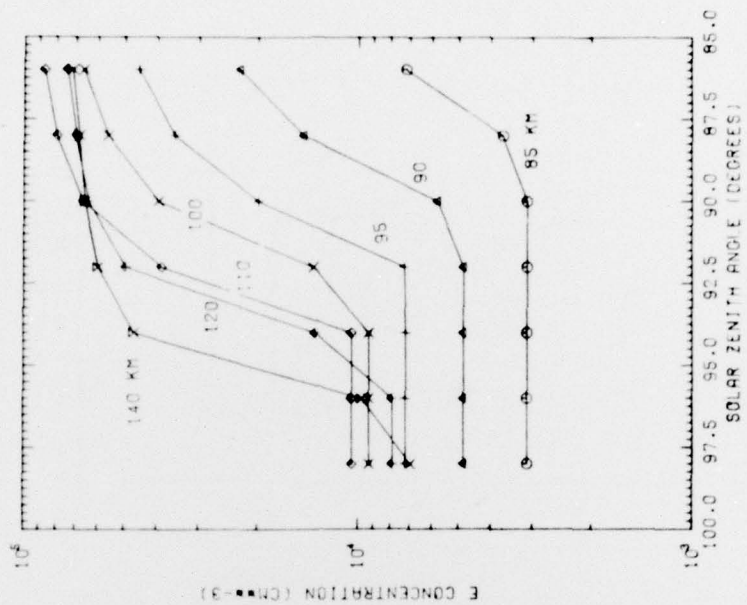


Figure 10d. Same as Figure 2b, Except NO Increased by a Factor of 10² and Absorption of HfLy α by NO Included

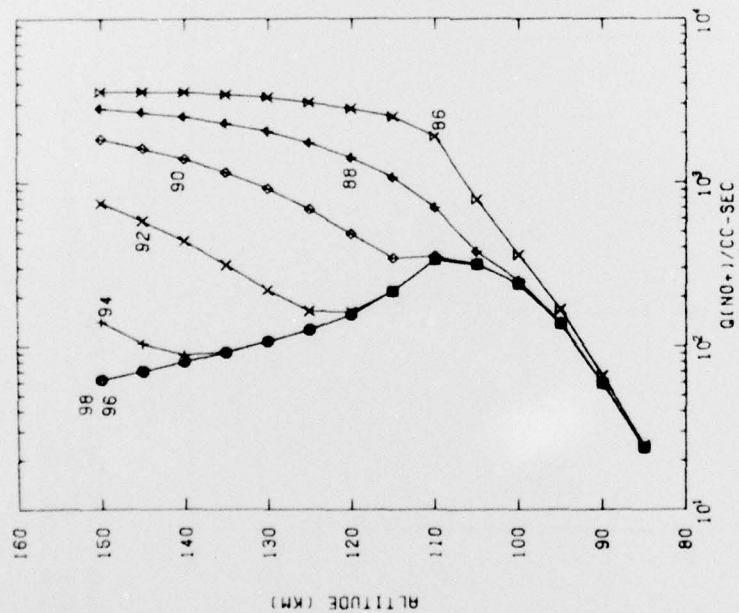


Figure 11a. Same as Figure 1a, Except NO Increased by a Factor of 10^3 and Absorption of $HL_{y\alpha}$ by NO Included

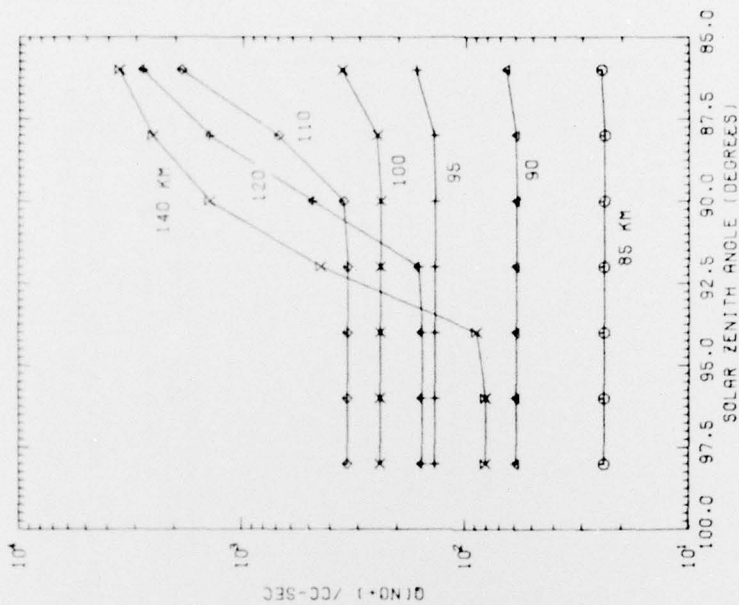


Figure 11b. Same as Figure 1b, Except NO Increased by a Factor of 10^3 and Absorption of $HL_{y\alpha}$ by NO Included

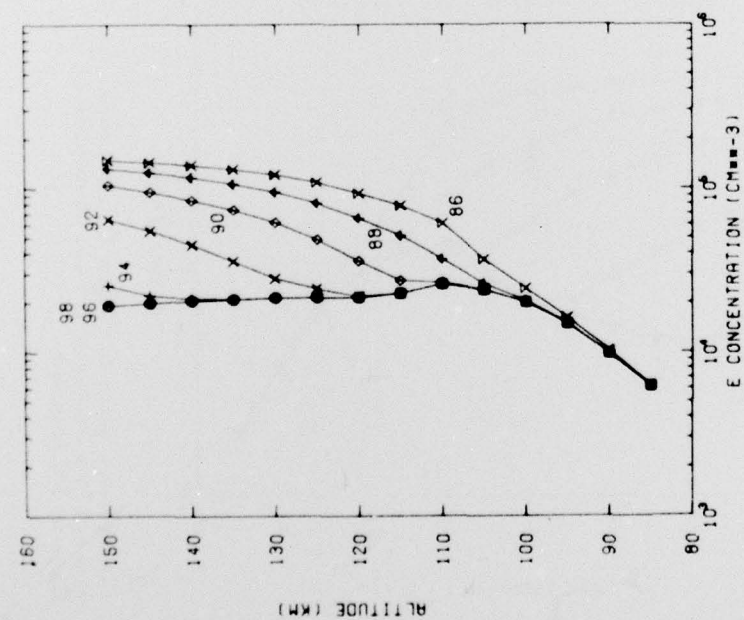


Figure 11c. Same as Figure 2a, Except NO Increased by a Factor of 10^3 and Absorption of $\text{HLY}\alpha$ by NO Included

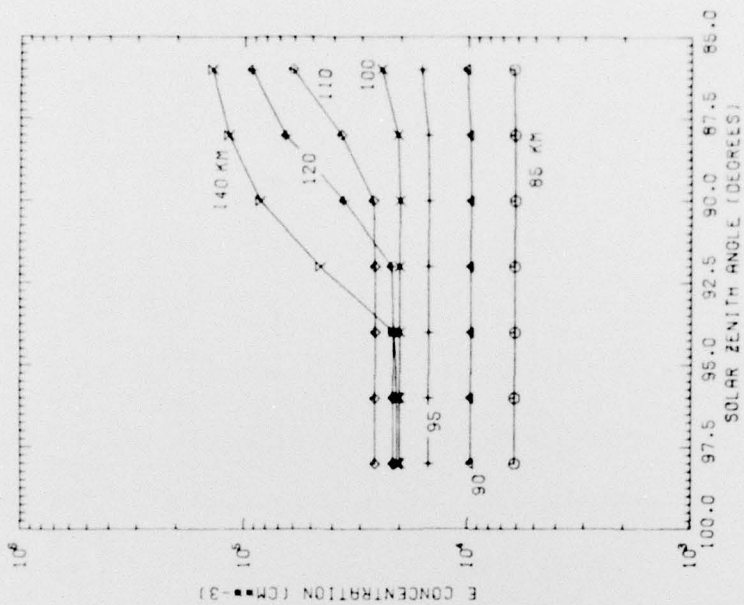


Figure 11d. Same as Figure 2b, Except NO Increased by a Factor of 10^3 and Absorption of $\text{HLY}\alpha$ by NO Included

References

1. Nicolet, M. (1965) Ionospheric processes and nitric oxide, J. Geophys. Res. 70:691-701.
2. Swider, W. (1965) A study of the nighttime ionosphere and its reaction rates, J. Geophys. Res. 70:4859-4873.
3. Meira, L.G., Jr. (1971) Rocket measurements of upper atmospheric nitric oxide and their consequence to the lower ionosphere, J. Geophys. Res. 76:202-212.
4. Keneshea, T.J., Swider, W., and Narcisi, R.S. (1970) E-region model, J. Geophys. Res. 75:845-854.
5. Rusch, D.W., and Barth, C.A. (1975) Satellite measurements of nitric oxide in the polar region, J. Geophys. Res. 80:3719-3721.
6. Strobel, D.F., Young, T.R., Meier, R.R., Coffey, T.P., and Ali, A.W. (1974) The nighttime ionosphere: E-region and lower F-region, J. Geophys. Res. 79:3171-3178.
7. Wakai, N. (1967) Quiet and disturbed structure and variations of the nighttime E-region, J. Geophys. Res. 72:4507-4517.
8. King, G.A.M. (1965) The aurora and night E-layer, J. Atmos. Terr. Phys. 27:426-428.
9. Zipf, E.C., Borst, W.L., and Donahue, T.M. (1970) A mass spectrometer observation of NO in an auroral arc, J. Geophys. Res. 75:6371-6376.
10. Swider, W., and Narcisi, R.S. (1977) Auroral E-region: Ion composition and nitric oxide, Planet. Space Sci. 25:103-116.
11. Hyman, E., Strickland, D.J., Julienne, P.S., and Stroble, D.F. (1976) Auroral NO₂, J. Geophys. Res. 81:4765-4769.